Er-doped ZnO films grown by pulsed e-beam deposition

2007 J. Phys.: Condens. Matter 19 266216

(http://iopscience.iop.org/0953-8984/19/26/266216)

J. Phys.: Condens. Matter **19** (2007) 266216 (7pp) doi:10.1088/0953-8984/19/26/266216

Er-doped ZnO films grown by pulsed e-beam deposition

Z Pan[1], S H Morgan[1], A Ueda[1], R Aga Jr[1], A Steigerwald[1], A B Hmelo[2] and R Mu[1]

[1] Physics Department, Fisk University, Nashville, TN 37208, USA
[2] Department of Physics and Astronomy, Vanderbilt University, Nashville, TN 37235, USA

E-mail: zpan@fisk.edu

Received 30 April 2007, in final form 21 May 2007
Published 15 June 2007
Online at stacks.iop.org/JPhysCM/19/266216

Abstract

Erbium (Er)-doped ZnO thin films were grown on fused silica (SiO_2) substrates by pulsed electron-beam deposition (PED) and analysed by Rutherford backscattering spectrometry (RBS), ultraviolet–visible absorption, and photoluminescence (PL). Subsequent annealing at 700 °C produces remarkable effects on the optical properties of Er-doped films. Under 325 nm excitation, a dramatic increase of deep-level emission from 450 to 680 nm was observed from annealed Er-doped ZnO films. Under 488 nm excitation, the PL spectrum of annealed Er-doped ZnO films revealed sharp and well-resolved Stark-splitting peaks in both the green emission of $^4S_{3/2} \rightarrow {}^4I_{15/2}$ transition and the red emission of $^4F_{9/2} \rightarrow {}^4I_{15/2}$ transition of Er^{3+} ions, which suggests that the Er ions have been incorporated inside the crystalline ZnO grains after thermal annealing.

(Some figures in this article are in colour only in the electronic version)

1. Introduction

Erbium-doped semiconductors are considered to be promising optical materials for opto-electronic devices [1–3]. Recently, ZnO has attracted increased attention as a candidate host material for Er doping. ZnO is a wide-band-gap semiconductor with an oxide phase, which is applicable to the excitation of Er. It also has a high electrical conductivity, which is essential for the realization of actual current-injection opto-electronic devices [4, 5]. Other notable properties of ZnO include a large exciton binding energy and a large Zn–O bond strength, which allows a high laser irradiation [6]. The Er-doped ZnO films have been fabricated using many techniques, including sintering [7], wet processing [8], ion implantation [9, 10], textured spraying [6], electron-beam evaporation [11], and pulsed-laser deposition (PLD) [4, 12, 13]. It has been reported that the emission of Er ions in ZnO films is inhomogeneously broadened,

similar to that in amorphous materials, suggesting that rare earths are accumulated at the grain boundaries of polycrystalline ZnO films [9, 14].

Material ablation by a pulsed electron beam (e-beam) is based on transient heating and evaporation. An e-beam with a pulsed width of 100 ns is generated by a commercial channel-spark source (PEBS-20) from Neocera Inc. Briefly, this source behaves similarly to a plasma diode. The discharge medium is a plasma, which connects the cathode (inside of the source) and the anode (outside of the source). Generation of the pulsed e-beam starts with triggering and ends as the conductivity of the entire plasma conductor becomes high enough to draw a large current from a capacitor bank, causing breakdown of the diode. During this process, electrons accelerate from the cathode plasma to the anode plasma, as facilitated by the charging potential. These electrons constitute the pulsed e-beam, which is delivered to the target via a dielectric channel with an inner diameter of around 3.2 mm. Thus, a high beam current density of the order of 10^6 A cm^{-2} can be achieved. The average electron energy can be adjusted from 8 to 20 keV by varying the charging potential of the channel-spark source. The total e-beam energy is transferred to the target with transfer efficiency of around 30% [15]. This is responsible for the transient local heating on the target that consequently leads to evaporation. The rate of temperature increase for the local spot is directly proportional to the power density of the incident e-beam and inversely proportional to the product of the target specific heat capacity, target density and thermal diffusion length. PED offers several unique advantages over PLD, such as high beam-to-target energy transfer efficiency and the ability to ablate materials with high optical transparency and reflectivity. The e-beam also promotes dissociation, excitation, and ionization of the fill gas, which could be utilized to form compounds such as oxides and nitrides. PED has been around since the early 1990s, but most of the applications have been for the fabrication of high-T_c superconducting cuprates. Only recently has it been employed to deposit zirconium tin titanate films ($ZrSnTiO_4$), zinc oxide films (ZnO), and tin oxide transparent conducting films (SnO_2) [16].

In this paper, we report on Er-doped ZnO films grown on fused silica substrates by PED followed by thermal annealing. We characterized films both before and after annealing using Rutherford backscattering spectrometry (RBS), ultraviolet–visible absorption, and photoluminescence (PL). The PL was measured at two excitation wavelengths 325 and 488 nm. The 325 nm (above-band-gap excitation) is used for exciting the host semiconductor ZnO, while 488 nm is used for directly exciting doped Er^{3+} ions in the ZnO film to the $^4F_{7/2}$ level. The luminescence spectrum from annealed Er-doped ZnO film revealed sharp and well-resolved peaks under 488 nm excitation, which suggest that Er ions in the ZnO host are surrounded by a crystal field of noncubic symmetry.

2. Experimental procedures

Er-doped ZnO films were grown on fused silica substrates by PED, using a Model PEBS-20 from Neocera Inc. The size ($L \times W \times T$) of the substrate is 8 mm × 8 mm × 1.5 mm. The deposition was performed under an oxygen pressure of 12 mTorr, with an electron energy of 19 keV, and a total of 20 000 shots at a pulse repetition rate of 2 Hz. Figure 1 shows a schematic layout of the PED system that was used. The distance between the target and the substrate is 45 mm. Four substrates were set at the centre of sample holder, with the front surface facing the target. The ablating target used in this work was a sintered pellet of a ZnO and Er_2O_3 mixture. The batch powders of 98.5 mol% ZnO and 1.5 mol% of Er_2O_3 were thoroughly mixed in an agate mortar. The mixed powders were then compressed using a hydraulic press to form a pellet; the pellet was further sintered at 1400 °C for 8 h to obtain the compact target. Thermal annealing of Er-doped film was performed at 700 °C in air for 2 h.

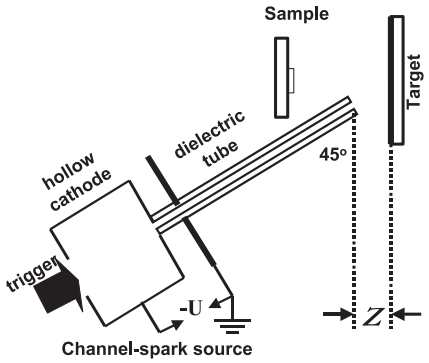

Figure 1. Schematic diagram of the pulsed electron-beam deposition system, which includes the channel-spark pulsed e-beam source, target, and substrate holder inside a vacuum chamber. The substrate holder is directly facing the target while the dielectric tube, which guides the e-beam towards the target, is oriented at 45° with respect to the target surface.

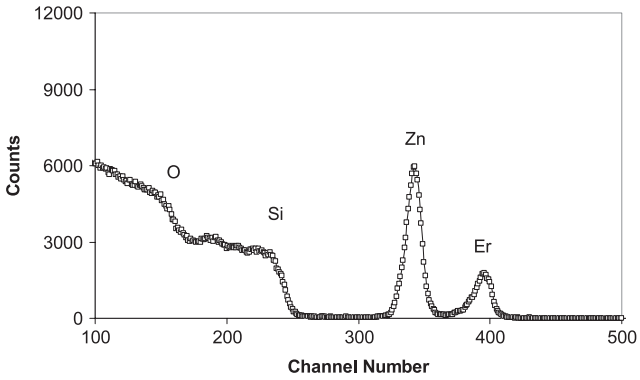

Figure 2. Rutherford backscattering spectrum with 1.8 MeV He^{2+} ions incident on Er-doped ZnO film grown under an oxygen pressure of 12 mTorr by pulsed electron-beam deposition.

The Rutherford backscattering spectra (RBS) was measured using 1.8 MeV He^{2+} ions at a scattering angle of 175°. UV–visible absorption of the films on fused silica was measured from 300 to 800 nm using a Cary dual-beam spectrophotometer.

Photoluminescence was measured at two laser excitation wavelengths. A HeCd laser (KIMMON model IK320R-D) at 325 nm was used as the above-band-gap excitation source, and an argon ion laser (Coherent Innova 90) at 488 nm was used for an Er^{3+} direct excitation source. The PL with 325 nm excitation was measured using an Oriel monochromator MS257™ with a thermoelectric (TE) cooled CCD detector, and the PL with 488 nm excitation was measured using a Spex Model 1403 double-grating spectrometer with a cooled RCA31034 PMT and a photon-counting system. The incident laser power that was used was 20 mW for a HeCd laser (the estimated intensity at the focus is about 3.0×10^4 W cm^{-2}) and 150 mW for an argon ion laser, respectively. The luminescence was measured at room temperature.

3. Results and discussion

Figure 2 shows the RBS profile of the annealed Er-doped ZnO film on a SiO_2 substrate. The profile of the as-deposited film is similar, suggesting that the oxygen deficiency is not

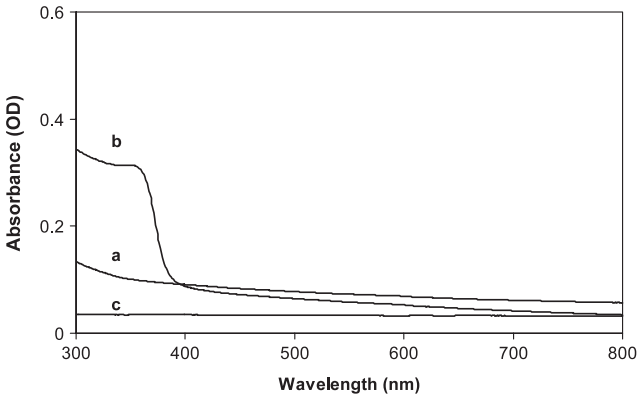

Figure 3. Optical absorption spectra of (a) Er-doped ZnO film, as-deposited; (b) Er-doped ZnO film, heat-treated at 700 °C for 2 h; (c) SiO_2 substrate.

significant, as the film was grown under an O_2 atmosphere. There are small differences in the film thickness between the four samples in a batch. The difference in integrated peak counts in RBS is within ±7% and the Er/Zn ratio is within ±2% for four samples in a batch. The stoichiometric ratio of Zn and Er was determined using the formula:

$$\frac{N_{\mathrm{Er}}}{N_{\mathrm{Zn}}} = \frac{A_{\mathrm{Er}}}{A_{\mathrm{Zn}}} \frac{\sigma_{\mathrm{Zn}}(E,\theta)}{\sigma_{\mathrm{Er}}(E,\theta)} \tag{3.1}$$

where A_i is the integrated peak count and $\sigma_i(E,\theta)$ is the cross section for compound i. The Er-doping level calculated using RBS data and equation (3.1) is 5.8 at.%. This Er-doping level in the film is significantly higher than that in a batch composition of target pellet, which is 3 at.%. The material in the deposited film came from very near the surface of the target pellet being ablated. The increased Er-doping level in film suggests that the surface layer of the target has a higher Er concentration than the batch composition. It has been reported that rare-earth ions in ZnO start to diffuse towards the surface at temperatures above 900 °C [17]. Therefore, an increase in Er concentration in the surface layer of the pellet is expected because of the high-temperature sintering process (1400 °C for 8 h). The film thickness was determined by comparing the integrated count of Zn peaks in the RBS of the film studied and that of the Zn peak in the RBS of a reference ZnO film with a known thickness, and by adding 8.1% for an estimated correction for the Er doping. This estimated correction is based on the Er concentration and the density ratio of ZnO/Er_2O_3. The thickness thus calculated is 130 ± 8 nm.

Figure 3 shows the UV–visible absorption spectra of (a) as-deposited, (b) heat-treated Er-doped films, and (c) the absorption of SiO_2 substrate as a reference. The annealed Er-doped ZnO film shows a sharp absorption edge at about 375 nm (3.3 eV). In contrast, the as-deposited Er-doped film shows a UV absorption tail extended to about 400 nm; the UV absorbance is significantly lower than that of the annealed film. The absorption spectra provide evidence for the formation of crystallized ZnO grains after annealing, because the sharp absorption edge at about 375 nm is an intrinsic property of ZnO crystal.

The PL spectra excited at 325 nm by a He–Cd laser are shown in figure 4 for the Er-doped film before and after annealing, and also for an undoped ZnO film grown by PED under the same conditions for comparison. The PL of as-deposited films show only an intense near-band-edge emission band peaked at 379 nm. However, the PL of annealed films shows two emission

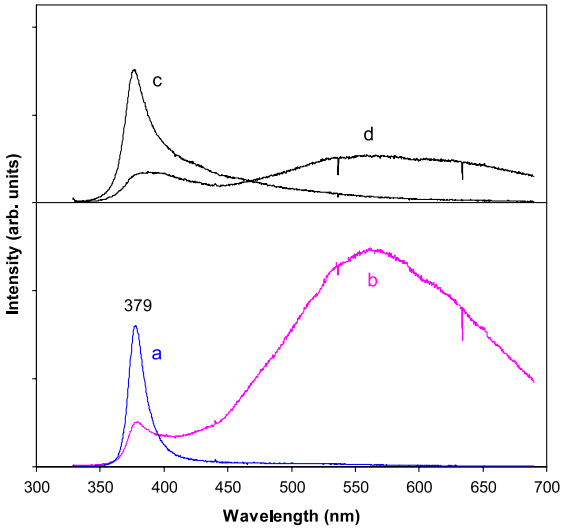

Figure 4. Room-temperature photoluminescence excited at 325 nm: (a) Er-doped ZnO film, as deposited; (b) Er-doped ZnO film, heat-treated at 700 °C for 2 h; (c) ZnO film, as deposited; (d) ZnO film, heat-treated at 700 °C for 2 h.

bands: a near-band-edge emission (NBE) peaked at about 380 nm and a visible broad band from 450 to 680 nm, attributed to deep-level emission (DLE) [18, 19]. The NBE is attributed to excitons of the ZnO crystal, while the DLE is attributed to defects and impurities [18, 19]. The annealing at 700 °C produced remarkable effects on activating DLE: the DLE increases, while the NBE decreases. The increase in DLE is much more significant for Er-doped ZnO film than that of ZnO film, as shown in traces (b) and (d) in figure 4. The peak intensity ratio of DLE to NBE is 4.9 for Er-doped ZnO film, compared to 1.5 for ZnO film. Therefore, Er doping plays a role in the remarkably increased DLE. Previous studies reported that the intentionally doped impurities could provide a significant contribution to DLE, for example by providing donor–acceptor pairs in ZnO [18, 19]. The majority of Er in ZnO is likely to be associated with rare earths occupying substitutional Zn sites [9], and the local lattice is modified because of the different oxidation states and ionic sizes of Er and Zn ions [5, 13, 20, 21]. The incorporation of Er ions in the ZnO lattice is therefore expected to increase the deep-level states. Annealing at 700 °C could allow the reorganization of the oxygen around Er ions and the growth of ZnO crystalline grains in the film, and therefore it could make deep-level states optically active. The PL results suggest that the generated electron–hole pairs (excitons) recombine non-radiatively by exciting deep-level states during 325 nm pumping, resulting in an increase in DLE and a decrease in NBE. Energy transfer might also occur between excitons and Er^{3+} ions [12], however we did not observe Er^{3+} emission peaks in the visible region. It might be possible that the weak emission peaks of Er^{3+} ions were embedded in the trace of a strong DLE.

The PL spectra excited at 488 nm are shown in figure 5 for the Er-doped film before and after annealing, and also for an Er-doped germanate glass sample with 2 mol% of Er_2O_3 for comparison [22–24]. The Er^{3+} emission is very weak for as-deposited film but significantly enhanced for annealed film. The intra-4f transition is forbidden in an isolated Er, but a crystal field produced by the ligands can make it allowed [21, 25]. Therefore, the reorganization of oxygen atoms around the Er ions by annealing could lead to a much stronger Er^{3+} emission [5, 13]. The green emission ranging from 540 to 564 nm can be identified with

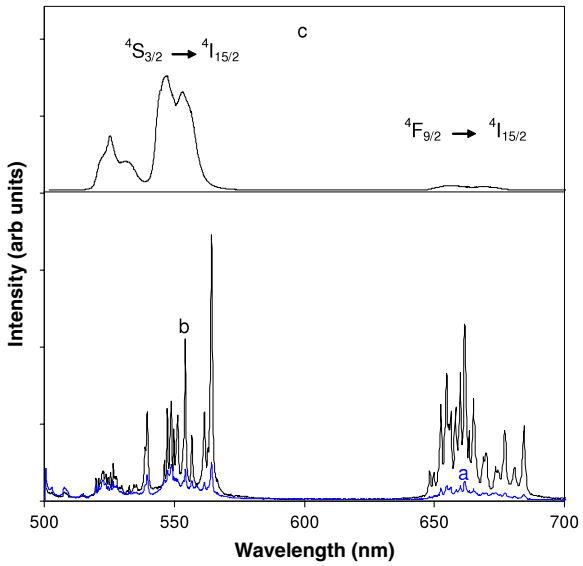

Figure 5. Room-temperature photoluminescence excited at 488 nm: (a) Er-doped ZnO film, as deposited; (b) Er-doped ZnO film, heat-treated at 700 °C for 2 h; and (c) Er-doped glass.

$^4S_{3/2} \rightarrow {}^4I_{15/2}$ transitions and the red emission ranging from 650 to 680 nm to $^4F_{9/2} \rightarrow {}^4I_{15/2}$ transitions of Er^{3+} ions [26–29]. As discussed by Shinn *et al* for optical transitions of Er^{3+} ions in $RbMgF_3$ crystal [29], the multiple sharp peaks in both green and red emission bands are the results of the splitting of the Er^{3+} energy level, when Er^{3+} ions sit in a crystal field without significant inhomogeneous broadening [3, 28, 29]. The $^4I_{15/2}$ multiplet can split into eight levels and $^4S_{3/2}$ to two levels in a single site by a non-cubic crystal field [29]. The abundant sharp peaks in spectrum 5(b) suggest that Er ions in the ZnO host are surrounded by a crystal field of non-cubic symmetry, and that it may have more than one site. In comparison, PL from Er-doped glass in figure 5(c) shows a smooth profile of emission, which is the results of the $^4I_{15/2}$ multiplet splitting combined with inhomogeneous broadening generally seen in an amorphous host [3, 28]. The well-resolved splitting feature of PL provides the evidence that the Er^{3+} ions are incorporated inside ZnO crystalline host after annealing [28, 29]. In figure 5(b), the red emission of $^4F_{9/2} \rightarrow {}^4I_{15/2}$ is quite intense, comparable to green emission of $^4S_{3/2} \rightarrow {}^4I_{15/2}$, while the red emission of $^4F_{9/2} \rightarrow {}^4I_{15/2}$ is much weaker relative to green emission of $^4S_{3/2} \rightarrow {}^4I_{15/2}$ in glass (figure 5(c)). According to our previous studies, a relatively increased red-to-green emission ratio is attributed to energy transfer between excited Er^{3+} ions [3, 22, 27]. In addition, the background of spectrum (figure 5(b)) is very weak, which indicates no significant energy transfer between excited Er^{3+} ions and deep-level states under 488 nm excitation.

4. Conclusion

We have, to our knowledge, fabricated the first Er-doped ZnO film using pulsed electron-beam deposition. Subsequent annealing at 700 °C produces remarkable effects on the optical properties of Er-doped film. We observed sharp and well-resolved emission peaks for Er^{3+} ions in ZnO film, which suggests that the Er ions have been incorporated inside the crystalline ZnO grains after annealing.

Acknowledgments

The authors would like to acknowledge professor L C Feldman of Vanderbilt University for his valuable technical discussion. This research is supported by US National Science Foundation NSF-CREST CA: HRD-0420516, NSF-STC CLiPS grant no. 0423914, and US Department of Defense (DOD)/ARO contracts: W911NF-05-1-0453 and W911NF-04-1-0400.

References

[1] Polman A and van Veggel F C J M 2004 *J. Opt. Soc. Am.* B **21** 871
[2] Wilson R G, Schwartz R N, Abernathy C R, Pearton S J, Newman N, Rubin M, Fu T and Zavada J M 1994 *Appl. Phys. Lett.* **65** 992
[3] Pan Z, Ueda A, Morgan S H and Mu R 2006 *J. Rare Earths* **24** 699
[4] Komuro S, Katsumata T, Morikawa T, Zhao X, Isshiki H and Aoyagi Y 2000 *Appl. Phys. Lett.* **76** 3935
[5] Ishii M, Komuro S, Morikawa T and Aoyagi Y 2001 *J. Appl. Phys.* **89** 3679
[6] Bubendorff J L, Ebothe J, El Hichou A, Dounia R and Addou M 2006 *J. Appl. Phys.* **100** 014505
[7] Park Y K, Han J I, Kwak M G, Yang H, Ju S H and Cho W S 1998 *Appl. Phys. Lett.* **72** 668
[8] Mais N, Reithmaier J P, Forchel A, Kohls M, Spanhel L and Müller G 1999 *Appl. Phys. Lett.* **75** 2005
[9] Wahl U, Rita E, Correia J G, Alves E, Araújo J P and The ISOLDE Collaboration 2003 *Appl. Phys. Lett.* **82** 1173
[10] Alves E, Rita E, Wahl U, Correia J G, Monteiro T, Soares J and Boemare C 2003 *Nucl. Instrum. Methods* B **206** 1047
[11] Zhang X T, Liu Y C, Ma J G, Lu Y M, Shen D Z, Xu W, Zhong G Z and Fan X W 2002 *Thin Film* **413** 257
[12] Komuro S, Katsumata T, Morikawa T, Zhao X, Isshiki H and Aoyagi Y 2000 *J. Appl. Phys.* **88** 7129
[13] Pérez-Casero R, Gutierréz-Llorente A, Pons-Y-Moll O, Seiler W, Defourneau R M, Defourneau D, Millon E, Perriére J, Goldner P and Viana B 2005 *J. Appl. Phys.* **97** 054905
[14] Bachir S, Azuma K, Kossanyi J, Valat P and Ronfard-Haret J C 1997 *J. Lumin.* **75** 35
[15] Jiang Q D, Matacotta F C, Konijnenberg M C, Mueller G and Schultheiss C 1994 *Thin Solid Films* **241** 100
[16] Aga R S, Cox C, Ueda A and Jackson E 2006 *J. Vac. Sci. Technol.* A **24** L11
[17] Rita E, Alves E, Wahl U, Correia J G, Monteiro T, Soares M J, Neves A and Peres M 2006 *Nucl. Instrum. Methods* B **242** 580
[18] Bethke S, Pan H and Wessels B W 1988 *Appl. Phys. Lett.* **52** 138
[19] Garces N Y, Wang L, Bai L, Giles N C, Halliburton L E and Cantwell G 2002 *Appl. Phys. Lett.* **81** 622
[20] Ishii M, Ishikawa T, Ueki T, Komuro S, Morikawa T, Aoyagi Y and Oyanagi H 1999 *J. Appl. Phys.* **85** 4024
[21] Zhou Z, Komori T, Yoshino M, Morinaga M, Matsunami N, Koizumi A and Takeda Y 2005 *Appl. Phys. Lett.* **86** 041107
[22] Pan Z, Morgan S H, Loper A, King V, Long B H and Collins W E 1995 *J. Appl. Phys.* **77** 4688
[23] Pan Z, Morgan S H, Dyer K, Ueda A and Liu H 1996 *J. Appl. Phys.* **79** 8906
[24] Pan Z and Morgan S H 1997 *J. Lumin.* **75** 301
[25] Polman A 1997 *J. Appl. Phys.* **82** 1
[26] Pan Z, Ueda A, Hays M, Mu R and Morgan S H 2006 *J. Non-Cryst. Solids* **352** 801
[27] Pan Z, Ueda A, Mu R and Morgan S H 2007 *J. Lumin.* **126** 251
[28] Shinn M D, Sibley W A, Drexhage M G and Brown R N 1983 *Phys. Rev.* B **27** 6635
[29] Shinn M D, Windscheif J C, Sardar D K and Sibley W A 1982 *Phys. Rev.* B **26** 2371